≋USGS

science for a changing world

Geologic Map of Precambrian Rocks, Rawhide Buttes West Quadrangle and Part of Rawhide Buttes East Quadrangle, Hartville Uplift, Goshen and Niobrara Counties, Wyoming

By W.C. Day, P.K. Sims, G.L. Snyder, A.B. Wilson, and T.L. Klein, *with a section on* Geochronology *by* Zell E. Peterman, Kiyoto Futa, and R.E. Zartman

1999

U.S. Department of the Interior
U.S. Geological Survey

CONTENTS

FIGURES

TABLES

INTRODUCTION

Detailed geologic mapping (scale 1:24,000) of Precambrian rocks in the Hartville Uplift, southeastern Wyoming (Day and others, 1994; fig. 1) following earlier regional geologic mapping (scale 1:48,000) by Snyder (1980) has shown that the Late Archean granite and supracrustal rocks (Whalen Group) of the Wyoming province (fig. 2) were deformed during three convergent (tectonic) events in the Early Proterozoic, extending from between ~2.1 Ga to pre-1.7 Ga (table 1). These events are recorded in the Guernsey quadrangle (Sims and others, 1997) (fig. 1) and are expressed in part in this map area. From oldest to
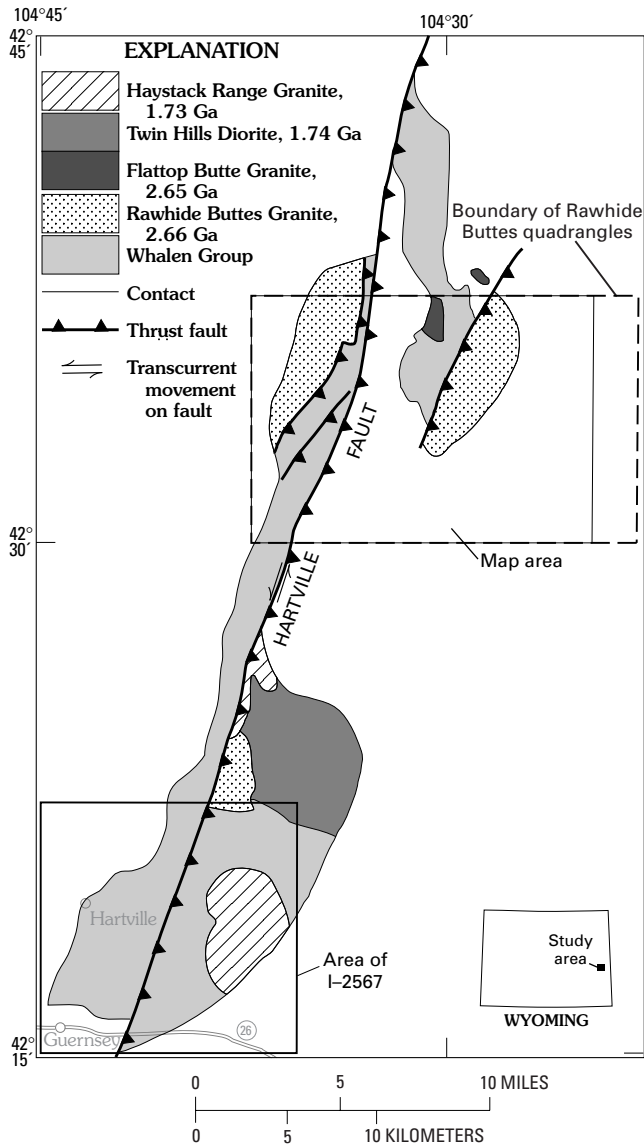
Figure 1. Index map of Hartville Uplift showing outline of Rawhide Buttes West and Rawhide Buttes East quadrangles. Outline of published map I–2567 (Sims and others, 1997) also shown.
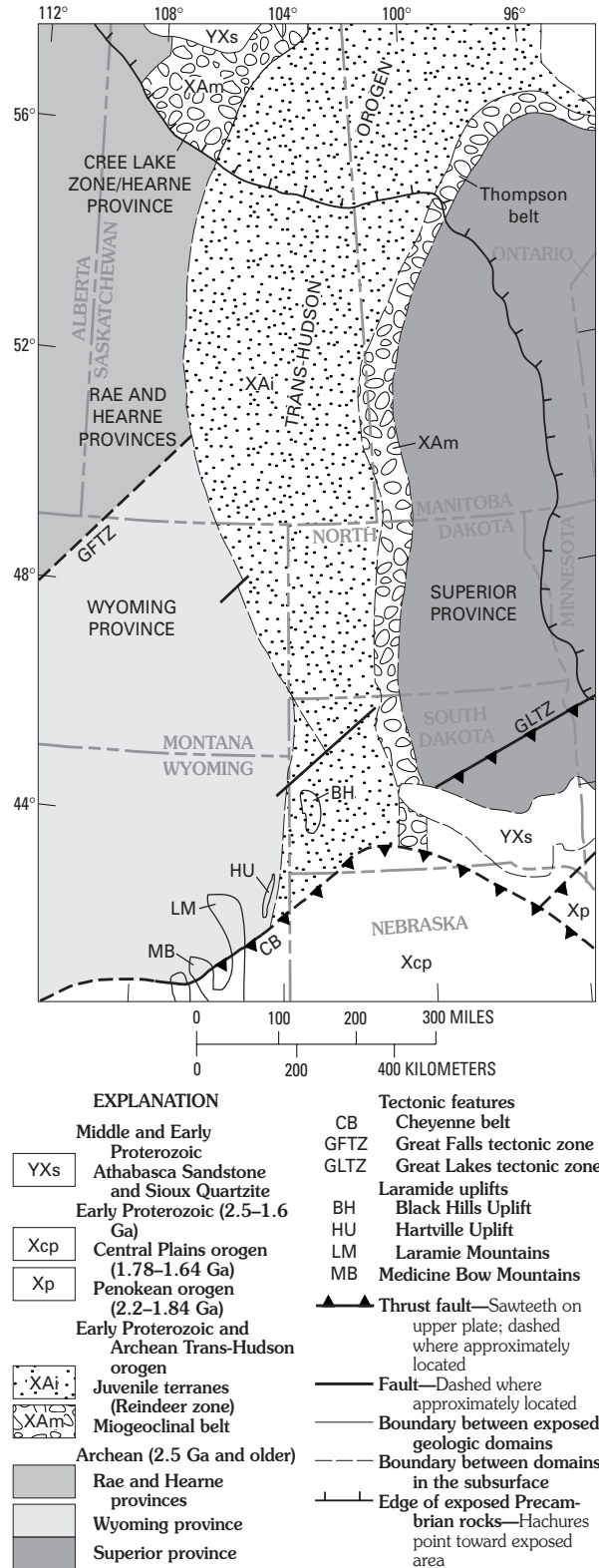
Figure 2. Precambrian basement map of north-central United States and adjacent Canada. The Hartville Uplift (HU) is at the intersection of the Trans-Hudson and Central Plains orogens, and rocks in the uplift were deformed by both Early Proterozoic orogenies, as well as by an earlier unnamed deformation (D$_2$).

1

Table 1. *Tectonic evolution of Hartville Uplift during the Precambrian.*

Age (Ga)	Event
1.32	Cryptic event indicated by biotite ages.
ca. 1.4	Emplacement of mafic dikes; undeformed.
ca. 1.6	Cryptic thermal event, indicated by sphene, apatite, and monazite.
1.72	Emplacement of Haystack Range Granite as domes, with deformed and metamorphosed margins—Deformation D_4.
1.74	Emplacement of Twin Hills Diorite as a predecessor to Haystack Range Granite.
	Deformation D_3—West-vergent fold-and-thrust belt on western continental margin of Trans- Hudson orogen; extends length of uplift.
2.1–1.98	Deformation D_2—Intense folding on east-west axes and accompanying metamorphism; south-vergent. Dated by Rb-Sr whole-rock and sphene methods on Flattop Butte Granite.
ca. 2.0	Emplacement of mafic dike swarm in rift fractures.
2.65	Crystallization of Rawhide Buttes and Flattop Butte Granite plutons.
	Deformation D_1—Nappe Formation
	Deposition of Whalen Group.
ca 3.0	Crystalline basement, indicated by Sm-Nd ages.

youngest, the deformation events are (1) inversion of supracrustal succession (deformation D_1), at least in parts of the uplift; (2) south-vergent folding of rocks on east-west axes (D_2) with concomitant prograde metamorphism; and (3) west-vergent folding on north-trending axes and accompanying thick-skinned thrusting with concomitant prograde metamorphism (D_3). A subsequent deformation event (D_4) was associated with post-tectonic intrusion of granites that resulted in doming of the supracrustal rocks. For the Guernsey quadrangle D_2 is attributed to an older, Early Proterozoic unnamed orogeny (~1.98 Ga), that produced fold nappe(s). Sims and others (1997) assigned the D_3 deformation to the Trans-Hudson orogeny (THO; fig. 2) (post-1.8 Ga; Lewry and others, 1996). However, the absolute age of the D_3 event is poorly constrained. To date, the effects of the 1.76-Ga Cheyenne Belt deformation, as recorded in the Laramie Range to the west and the Medicine Bow Mountains to the southwest (Resor and others, 1996) on the rocks of the Hartville Uplift are unknown. However, the orogenic front, as preserved in the Cheyenne shear zone, projects under the Phanerozoic sediments only about 20 km to the east and could have affected the Precambrian rocks exposed in the Hartville Uplift. The fourth deformation (D_4) observed on the eastern side of the map area resulted from doming caused by emplacement of bodies equivalent to the 1.72-Ga Haystack Range Granite.

The Precambrian episodes of deformation expressed in the Rawhide Buttes area are similar to those in the Guernsey area. Two regional deformations (D_2 and D_3) are recognized in the Rawhide Buttes East and Rawhide Buttes West 1:24,000 quadrangles. They compose a fold-and-thrust belt (D_3) on the western, continental margin of the Trans-Hudson orogen. A generally prominent ductile S-surface (S_3) containing a stretching lineation (L_3) is present locally. The stretching lineation (X direction of the strain ellipsoid) plunges moderately southeast, indicating a northwest direction of tectonic transport (see map) during deformation D_3. Deformation D_2 affected the entire uplift. It was a compressional deformation characterized by south-vergent folds. D_4 resulted in the formation of mullion structures and strong gneissic foliation in the margin of ~1.7-Ga plutons as well as a doming of the supracrustal rocks adjacent to the plutons.

Since publication of map I–2567 (Sims and others, 1997), the Precambrian geology of the Guernsey and Casebier Hills quadrangles, in the southern part of the Hartville Uplift, we have determined that the layered supracrustal rocks throughout the Hartville Uplift, assigned to the Whalen Group, are Late Archean. On the earlier published map, we classified these rocks as being either Early Proterozoic or Late Archean. The Flattop Butte Granite, previously thought to date from 1.98 Ga but now known to be Late Archean (2.65 Ga), cuts and intrudes the layered rocks. Also, on the earlier map, we erroneously considered the Rawhide Buttes Granite as basement to the Whalen Group. Instead, the basement is an unidentified crystalline sequence (>2.8 Ga), as indicated by Sm-Nd isotopic data (see table 5).

In this report, we use informal lithologic names to describe the supracrustal rocks of the Whalen Group (Smith, 1903). We propose the formal name "Rawhide Buttes Granite" for the bodies of granitic rocks exposed at Rawhide Buttes (type area) and Rawhide Creek, west of the Hartville fault. This rock unit was previously called "Granite of Rawhide Buttes" by Snyder (1980). We also propose that the Granite of Flattop Butte of Snyder (1980) be formally named "Flattop Butte Granite."

The term "terrane" is used herein in the same way as in the North American cordillera (Jones and others, 1977). It comprises a distinctive crustal segment characterized by a unique stratigraphy and structural style and is fault bounded.

STRATIGRAPHY

The stratigraphy of rocks of the Whalen Group in the quadrangles was determined from exposures along the south-plunging, asymmetrical anticline south of Flattop Butte. Elsewhere in the map area, contacts are mostly ductile faults. The structurally oldest rocks exposed in the anticline

are garnet-biotite schist (unit Ws_1) adjacent to the Flattop Butte Granite, which intrudes the layered rocks in the anticline. The schist is amphibolite facies, containing biotite, garnet, and sillimanite. The schist contains layers and lenses of quartzite (unit Wq_1). Kyanite is present locally just north of this map area in the Silver Springs quadrangle. Structurally overlying the schist is a metacarbonate unit composed predominantly of metadolomite (unit Wd) that contains lenses of banded iron-formation (unit Wif), pelitic schist (unit Wps), quartz-pebble metaconglomerate (unit Wc), and metaquartzite (unit Wq). The metadolomite locally contains tremolite and chondrodite. Overlying the metadolomite is another, thicker(?) unit of biotite-muscovite schist (unit Ws_2), which is garnetiferous and, locally, sillimanitic, contains pseudomorphs of staurolite, and lacks the extensive interlayers of clastic metasediments. Snyder (1980) recognized graded beds in the schist (unit Ws_2) on the poorly exposed west limb of the anticline, which support the structural facing of the dolomite (unit Wd) and schist units. The contacts between the metasedimentary units and the mafic metavolcanic rocks (unit Wmv) in the area are faulted where exposed. However, the mafic metavolcanic rocks are presumed to be the youngest unit of the Whalen Group in the area. This would be consistent with stratigraphic relationships in the Guernsey quadrangle (Sims and others, 1997).

Where exposed east of the Hartville fault, the succession is believed to be upright, whereas the succession exposed in Muskrat Canyon, on both the hanging and footwall plates of the Muskrat Canyon fault, appears to be inverted. West of the Muskrat Canyon fault, crossbedded quartzite (NW¼ sec. 24, T. 30 N., R. 65 W.) indicates overturned beds, and east of the fault basalt pilllows (N½ sec. 19, T. 30 N., R. 64 W.) are overturned.

At Bald Butte, the Archean Rawhide Buttes Granite (unit Wr) clearly intruded metadolomite, conglomeratic pelitic schist, quartzite, and layered amphibolite of the Whalen Group. Although the granite-metasediment contacts are conformable at this locality because of infolding, some of the metasedimentary rocks are migmatized near granite contacts, indicating that they are older than the granite.

The Whalen Group is older than the ~2-Ga metadiabase; the mafic dikes cut all rock units of the Whalen Group.

GRANITIC ROCKS

The two principal granitic rock types in the area, Rawhide Buttes Granite (unit Wr) and Flattop Butte Granite (unit Wfb), differ in lithology and can be distinguished in the field. The Rawhide Buttes Granite is a two-mica biotite granite; both muscovite and sillimanite are present locally. It ranges in composition (fig. 3) from granodiorite to a potassic granite (table 2), but is mainly granite in the strict sense. Three separate bodies are delineated in the map area—the Rawhide Buttes body (type area), the Bald Butte

body, and the Rawhide Creek body. The granite in the Rawhide Creek body is partly mylonitic gneiss. Like the Flattop Butte Granite, the Rawhide Buttes Granite is similar in mineralogy and geochemistry (unpub. data, 1997) to S-type granitoids (see Chappell and White, 1974, 1992).

The two-mica Archean Flattop Butte Granite differs from the 2.66-Ga Rawhide Buttes Granite (see below) in being finer grained, more equigranular, in containing ubiquitous muscovite, and in being lighter in color (pinkish gray to gray) in outcrop. There are several horizons of coarse tourmaline-garnet-muscovite-biotite pegmatite interlayered in the supracrustal rocks immediately adjacent to the main body of the Flattop Butte Granite on the south side of Flattop Butte, which may be apophyses related to the main body. These apophyses were included in map unit Wfb. The Flattop Butte Granite (unit Wfb) and its country rock were deformed during deformations D_2 and D_3. The Flattop Butte Granite is a biotite-muscovite granite. On a K-Q-P diagram (fig. 3) all samples plot in the granite field. Table 3 lists the modal composition (volume percent) of four samples. Like the Rawhide Buttes Granite, the Flattop Butte Granite is chemically similar to S-type granitoids (Chappell and White, 1974, 1992; Ferguson and others, 1980), which are generally interpreted as resulting from partial melting of peraluminous sedimentary rocks (as distinct from I-type granitoids, which have an igneous source).

STRUCTURE

The map area composes a part of the southeastern margin of the Wyoming Archean craton. An early nappe-forming
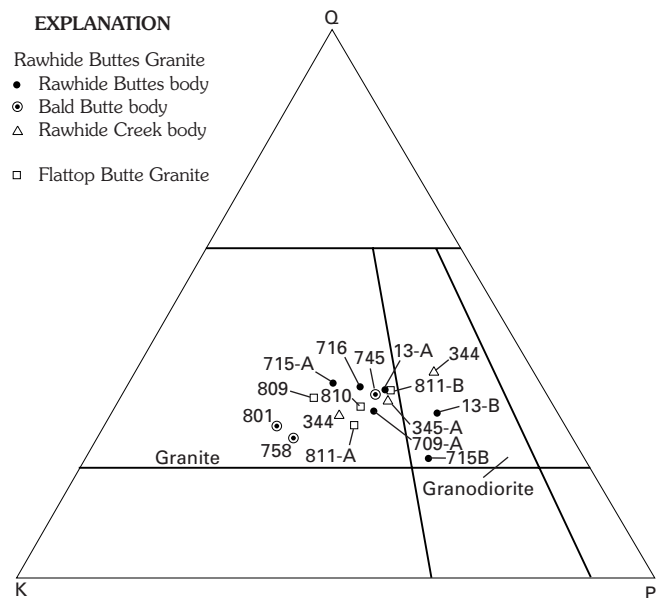

Figure 3. K-Q-P diagram showing compositions (volume percent) of 2.65-Ga Flattop Butte Granite and 2.66-Ga Rawhide Buttes Granite. These granitic units have comparable compositions.

Table 2. *Approximate modes of Rawhide Buttes Granite (percent by volume).*

[Tr, trace amounts present]

Sample No.	709A	13A	13B	715A	715B	716	745	758	801	344	345A	346
	Rawhide Buttes body						Bald Butte body			Rawhide Creek body		
Plagioclase	37.6	36.4	46.2	29.4	49.6	35.0	37.4	29.0	25.4	43.8	39.6	36.4
Quartz	30.7	30.4	28.8	32.6	19.4	33.0	31.8	24.4	26.2	35.4	30.4	28.4
Potassium feldspar.	23.6	22.0	18.4	29.8	22.2	27.0	25.6	42.2	43.0	14.2	23.6	32.4
Biotite	7.9	11.0	6.6	8.2	8.6	4.8	4.8	4.4	4.6	6.6	6.4	2.6
Accessory minerals.	0.2	0.2	Tr	Tr	0.2	0.2	0.4	Tr	0.8	Tr	Tr	0.2

Table 3. *Approximate modes of Flattop Butte Granite (percent by volume).*

[Tr, trace amounts present]

Sample No.	809	810	811A	811B
Plagioclase	28.4	36.4	37.0	39.4
Quartz	30.2	30.4	25.8	32.6
Potassium feldspar	33.8	26.2	31.0	22.8
Biotite	4.6	5.2	3.2	3.4
Muvcovite	3.0	1.8	3.0	1.8
Accessory minerals	Tr	Tr	Tr	Tr

episode of deformation (D_1) affected rocks in the southern part of the Hartville Uplift. Manifestation of D_1 in the northern part of the uplift is difficult to document. However, the entire uplift, at least on the western side, was deformed by an older, unnamed Proterozoic orogeny (D_2).

DEFORMATIONS D_1 AND D_2

Pre-D_3 deformational structures are present throughout the map area in both the layered supracrustal rocks of the Whalen Group and the granitic bodies. A strong schistosity (S_2), locally accompanied by a lineation given by aligned biotite and elongated garnet porphyoblasts, is ubiquitous. These structures are folded by F_3. The presence of D_2 structures in the area indicates that D_2, and also D_1, extend throughout the length of the uplift. The existence of D_1 is indicated by overturned beds in Muskrat Canyon, and possibly elsewhere. D_1 and D_2 were originally distinguished in the southernmost part of the uplift in the region near the Chicago iron mine near Hartville (Sims and others, 1997), which was not influenced by deformation D_3.

D_2 structures (S_2, L_2) are the dominant internal structures in the Archean Flattop Butte Granite. These structures have been folded by small- to large-scale, open, generally south-plunging F_3 folds. F_3 folds also determine the outline of the granitic body inasmuch as the granite and the country rock were folded together by F_3.

Deformation D_2 has been dated by the Rb-Sr whole-rock method on the Flattop Butte Granite at 1.98 Ga (see section by Peterman and others below). The deformation of the granite was pervasive and strong, and it yielded a tightly controlled Rb-Sr isochron.

DEFORMATIONS D_3 AND D_4

Deformation D_3 produced a north-trending fold-and-thrust belt that is parallel to the axis of the uplift and spans the length of it. The faults depicted on the map as thrusts are zones of ductile and, locally, cataclastic deformation and are interpreted to be thrust faults. The principal thrust(?), the Hartville fault, juxtaposes middle to upper amphibolite facies rocks to the east with upper greenschist facies rocks to the west. The estimated relative uplift of the eastern block is about 5 km (K.R. Chamberlain, University of Wyoming, oral commun., 1993). Where exposed in the Hell Gap quadrangle, the Hartville fault is a nearly vertical, 100-m-wide mylonite zone that has a steep stretching lineation and a late component of sinistral strike-slip offset. The fault is presumed to flatten to the east with depth, as a sled-runner type thrust.

D_3 folds trend north, verge westward, range from recumbent to steep, and generally plunge gently, either to the north or south. The recumbent folds have both dextral and sinistral asymmetries. D_3 folds are best exposed in the Wildcat Hills, in the southwestern part of the map area, and in the southern part of the Flattop Butte terrane (fig. 4). Exposures of these rocks in the Wildcat Hills extend southward a distance of 18 km, from Muskrat Canyon to the latitude of the Chicago mine (Sims and others, 1997). The direction of plunge of the folds, both to the north and south, is the result of superposed folding on older, east-west-trending, generally open D_2 folds.

Strain partitioning is particularly high in the D_3 thrusts, such as in the Muskrat Canyon and Little Wildcat Canyon fault zones (fig. 4). In fact, the occurrence of strong stretching lineation in the area is commonly a guide to the proximity of a thrust fault. However, high strain zones also are present locally in the rockmass between major thrust faults. An excellent example is the Rawhide Buttes granite in the
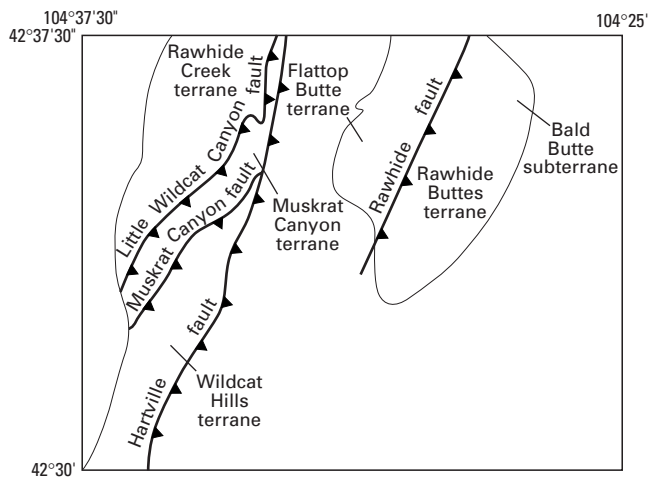
4

Figure 4. Index to tectonostratigraphic terranes in Rawhide Buttes West and Rawhide Buttes East quadrangles.

southern part of Rawhide Buttes. With few exceptions, the stretching lineations in the map area plunge at a moderate angle within a few degrees of S. 45° E., indicating northwest tectonic transport during D_3 deformation.

The absolute age of the D_3 deformation, which has been previously ascribed to the Trans-Hudson orogen (Sims and others, 1997) is poorly known for the Hartville Uplift. In the Black Hills of South Dakota, Redden and others (1990, 1996) have constrained the age of deformation to between 1.85 and 1.75 Ga. Recently, Dahl and Frei (1998) assigned a date of ~1.76 Ga for peak metamorphism from syntectonic metamorphic mineral pairs from a metapelite from the Black Hills. They employed a $^{207}Pb/^{206}Pb$ stepwise-leaching technique on garnet, staurolite and garnet-staurolite pairs and reported ages for these minerals of 1,762±15 Ma. 1,759±8 Ma, and 1,760±7 Ma, respectively. They also noted that the 1,760±7-Ma date closely correlates with the age of deformation associated with the Central Plains orogen (Sims and others, 1991), which represents a post-Trans-Hudson orogenic event that had a northwest vergence in this part of southeastern Wyoming and South Dakota. This age is similar to that of deformation recorded along the 1,780- to 1,740-Ma Cheyenne belt suture reported by Resor and other (1996), which is a suture associated with the Central Plains orogen. Therefore, D_3 in this part of the Hartville Uplift could be correlated with either the ~1.85- to 1.75-Ga Trans-Hudson orogen or the ~1.76-Ga deformation related to the Central Plains orogen as locally recorded in the Cheyenne belt suture zone deformation in the Medicine Bow Mountains of southeastern Wyoming.

To the south of this map area in the southern part of the Hartville Uplift the 1.74-Ga Twin Hills Diorite and the 1.72-Ga Haystack Range Granite intrude the supracrustal rocks, warping D_3 structures into structural domes (Sims and others, 1997). In the case of the Twin Hills Diorite,

mineral foliations wrap around the margin of the intrusion, indicating that they are flow foliations conformable to the outline of the body. Therefore, the D_3 deformation preceded emplacement of these intrusive bodies, which formed domal structures during the D_4 deformation. Later (D_4?) ductile shear zones cut the Twin Hills Diorite as linear through-going zones. Redden and others (1990) described a similar style of intrusion and deformation related to the 1.71-Ga Harney Peak Granite exposed in the Black Hills of South Dakota.

Krugh and others (1996) reported a U-Pb zircon age of approximately 1,715 Ma for a pegmatitic dike that intruded an amphibolite dike that cuts the granite on the eastern side of Rawhide Butte. They contended that the pegmatite was intruded during a folding event. R.L. Bauer (University of Missouri, oral commun., 1997) described a penetrative fabric in the pegmatite. These workers assigned the fabric in the pegmatite to be coeval with the peak metamorphism that affected the amphibolite dike, which they designated as a D_3 event. However, inasmuch as this is approximately the age of intrusion and deformation related to the 1.72-Ga Haystack Range Granite and other granitic rocks on the eastern side of the Hartville Uplift, a post-1.72-Ga age for D_3 is equivocal. The deformation they described may in fact be an event younger than D_3, and possibly related to the 1.72-Ga D_4 intrusive and folding event.

TERRANES DELINEATED IN MAP AREA

Five tectonostratigraphic terranes bounded by presumed thrust faults of deformation D_3 have been delineated in the map area. Two terranes are east of the Hartville fault and three are west of the fault (fig. 4). Those east of the Hartville fault—the Rawhide Buttes and Flattop Butte terranes—comprise deeper seated, higher grade crustal rocks than those west of the fault—Rawhide Creek, Muskrat Canyon, and Wildcat Hills terranes. The rocks east of the Hartville fault are predominantly sillimanite + kyanite bearing amphibolite facies, whereas those west of the fault are mainly greenschist facies. On the basis of the metamorphic mineral assemblage, the relative uplift of the eastern (hanging wall) block is estimated at about 5 km (K.R. Chamberlain, University of Wyoming, oral commun., 1993). Where exposed in the Hell Gap quadrangle, which is south of this map area (fig. 1, western segment of map I–2567, Sims and others, 1997), the Hartville fault is a high-angle, ductile reverse shear zone that dips steeply east and has a component of sinistral strike-slip offset. S-C mylonite, L-S tectonite, and S tectonite as much as 100 m wide mark the fault zone. The fault is presumed to flatten with depth. Mesoscopic evidence indicates that the fault has been active at least twice, with an early ductile component that caused the deformation cited above, and a later mylonitic episode.

5

Later narrower zones and veins of mylonite, which formed at the ductile-brittle transition, cut the earlier ductile fabrics in the fault zone. Movement, at least in part, is ascribed to the D_3 deformation; however, subsequent deformation has occurred along the fault.

RAWHIDE BUTTES TERRANE

The easternmost terrane in the map area, the Rawhide Buttes terrane (fig. 4), consists mainly of Rawhide Buttes Granite (unit Wr), which contains inclusions of older supracrustal Whalen Group rocks and is cut by a variable but predominantly north-trending mafic dike swarm (unit Xm). The dikes, as well as the country rock, were metamorphosed to amphibolite grade during D_2 and D_3 deformations, but were not noticeably folded.

The Rawhide Buttes Granite has a strong, steep, north-trending foliation (fig. 5A). The predominant foliation in the Rawhide Buttes Granite is interpreted to be a D_2 fabric, which was subsequently refolded into broad open folds during D_3 deformation. Additionally, the foliation has been reoriented into its present steeply dipping orientation during the westwardly directed D_3 thrusting. The L_3 stretching lineations (fig. 5B) were developed during the D_3 event. In the most northern part, the predominant lineation throughout the pluton is a generally north plunging mineral lineation (fig. 5B), that is parallel to rare fold axes. In the southernmost part of the pluton, the rock is gneissic in part and the predominant lineation is a stretching lineation (L_3). L_3 plunges moderately about S. 40° E., and represents the X-axis of the tectonic finite strain ellipsoid (fig. 5B). An older compositional layering in the granite probably represents original flow banding developed during emplacement of the granite in the Late Archean or layering developed during D_2 deformation.

The southeast-plunging stretching lineation in the gneissic Rawhide Buttes Granite indicates that the Rawhide Buttes terrane moved to the west-northwest relative to the adjacent Flattop Butte terrane during deformation D_3, inasmuch as the stretching lineation is assumed to indicate the direction of tectonic transport. Therefore, the moderate angle of plunge of L_3 indicates that the Rawhide Buttes terrane moved upward to the west-northwest and overrode rocks of the Flattop Buttes terrane along the Rawhide thrust fault.

An isolated butte, Bald Butte, which is 1.5 km north of Rawhide Buttes, is included in the Rawhide Buttes terrane, as the Bald Butte domain (or subterrane) because it lies in the hanging wall of the Rawhide fault (fig. 6). It differs from the Rawhide Buttes segment in structural attitude; the supracrustal rocks are infolded with the Rawhide Buttes Granite, and both trend northwest, presumably as a consequence of refolding on northwest axes during D_4 doming around a buried 1.73-Ga granite pluton north of Bald Butte. S_3 foliation (fig. 6A) strikes west-northwest and dips steeply

Figure 5. Equal-area projections (lower hemisphere) of structures in Rawhide Buttes Granite in Rawhide Buttes terrane (fig. 4). *A*, poles to S_2 foliation. *B*, orientation of L_3 lineations in the Rawhide Buttes Granite.

south. A stretching lineation (L_4?, fig. 6B) plunges moderately southwest adjacent to the buried dome.

FLATTOP BUTTE TERRANE

The Flattop Butte terrane, immediately west of the Rawhide Buttes terrane (fig. 4), is composed mainly of rocks of the Whalen Group, which are intruded by the Flattop
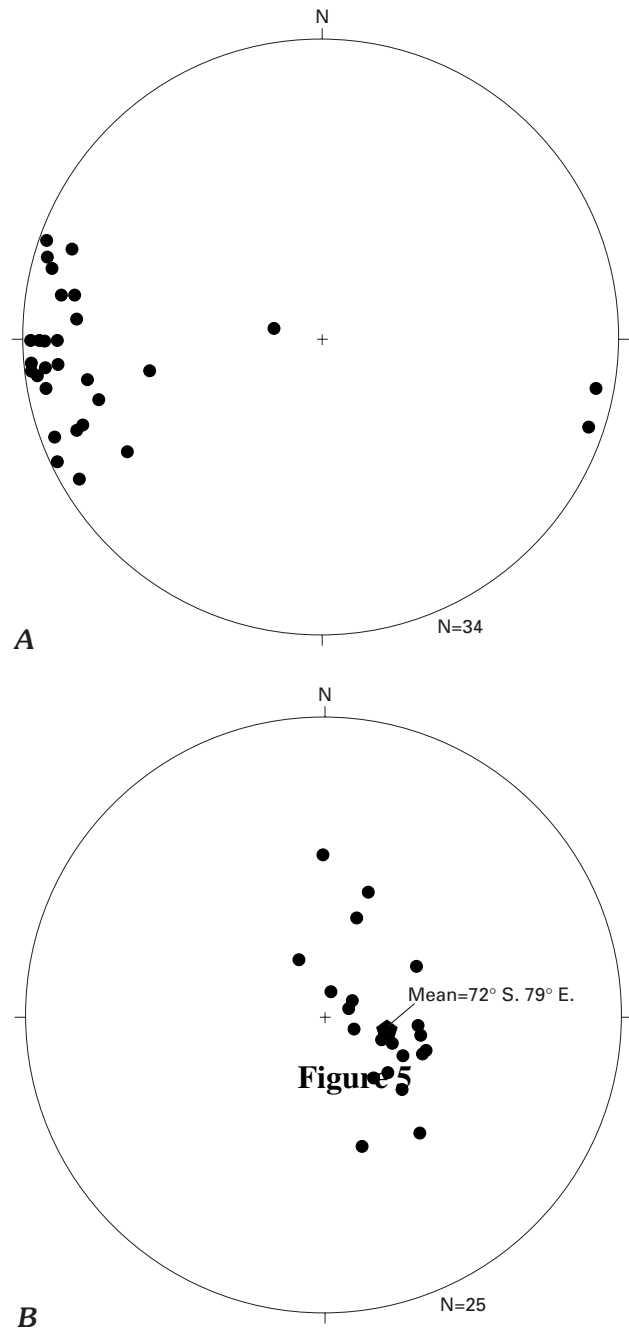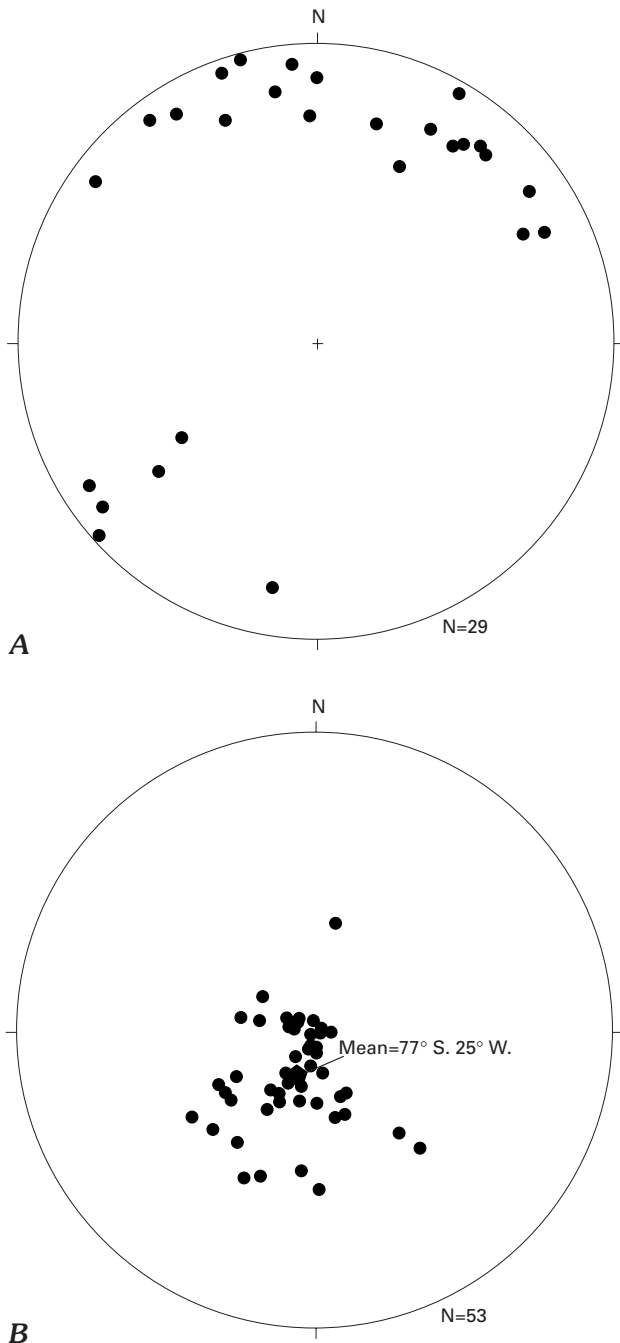
A

N=29

B

Mean=77° S. 25° W.

N=53

Figure 6. Equal-area projections (lower hemisphere) of structures in Bald Butte domain of Rawhide Buttes terrane (fig. 3). *A*, poles to foliation; foliations have been largely reoriented by D_5 doming. *B*, orientation of lineations.

Butte Granite. The terrane is bounded on the east by the Rawhide thrust fault and on the west by the Hartville fault. Structural elements for the metasedimentary rocks are plotted on stereographic nets in figure 7.

The predominant structure in this terrane is an asymmetric overturned anticline that verges to the west. A
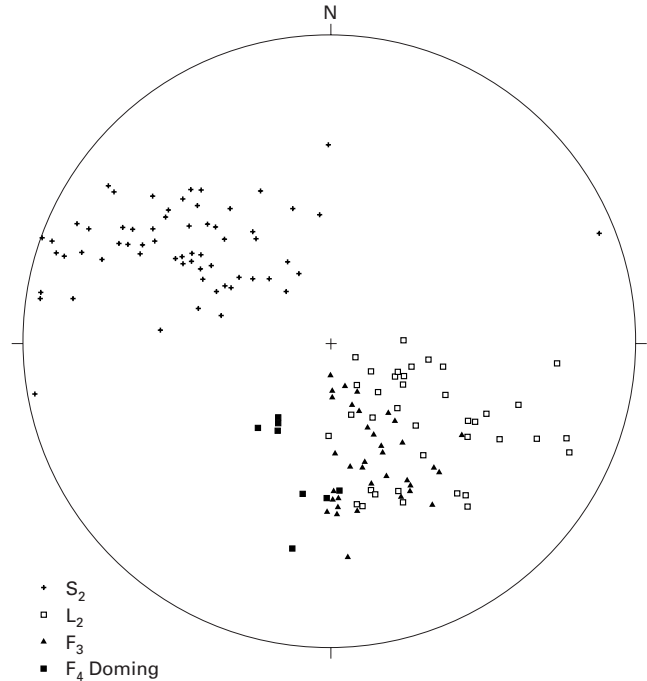

+ S_2
□ L_2
▲ F_3
■ F_4 Doming

Figure 7. Equal-area projection (lower hemisphere) of structures in southern part of Flattop Butte terrane (fig. 4). Measurements are on metasedimentary rocks.

schistosity (ductile) (S_2) is the main structure in the rocks; it mainly strikes north-northeast and dips east. The mean plunge of F_3 fold axes is 49°, S. 15° E., subparallel to the plunge of the major anticline. The rocks directly below, and west of, the Rawhide fault comprise an imbricate thrust sheet composed of thin wedges of diverse sedimentary-volcanic lithologies.

In the northernmost exposures in the map area (secs. 35, 36, T. 31 N., R. 64 W.), a stretching lineation in quartzite lenses within unit Wps plunges 40°–60°, S. 8°–20° E., roughly parallel to the plunge of F_3 folds in the terrane; the stretching lineation is not pervasive. This lineation differs from the direction of tectonic transport in most rocks of the Flattop Butte terrane during deformation D_3 . In the vertical plane, movement was upward to the northwest; this direction of tectonic transport is comparable, but different in detail, from that in the Rawhide Buttes terrane.

The Flattop Butte Granite (fig. 8), as well as the supracrustal rocks of the Whalen Group, were deformed during both D_2 and D_3. The northern and southern contacts of the body and internal foliations and lineations are subparallel to foliation and lineation in the adjacent country rock (Whalen Group), as a result of D_3 deformation.

RAWHIDE CREEK TERRANE

The Rawhide Creek terrane is on the west side of the Hartville fault (fig. 4) and is composed mainly of Rawhide Buttes Granite (unit Wr). The terrane is bounded on the east by the ductile Little Wildcat Canyon fault. The granite in the
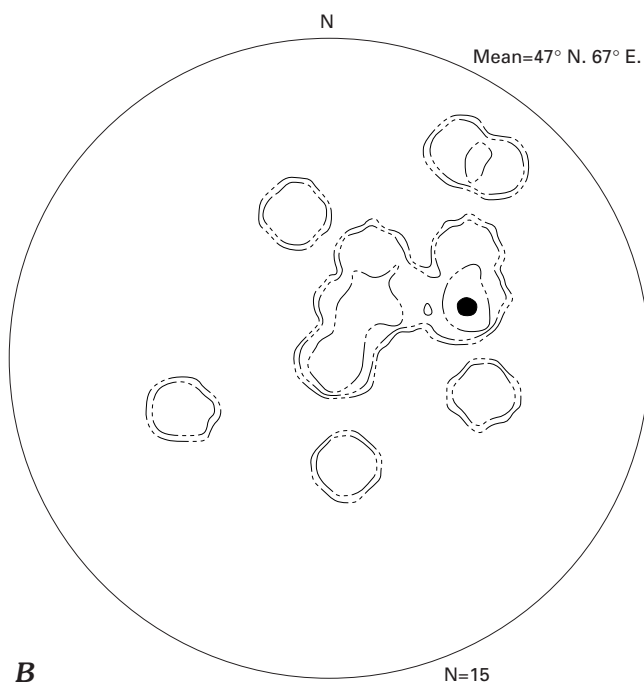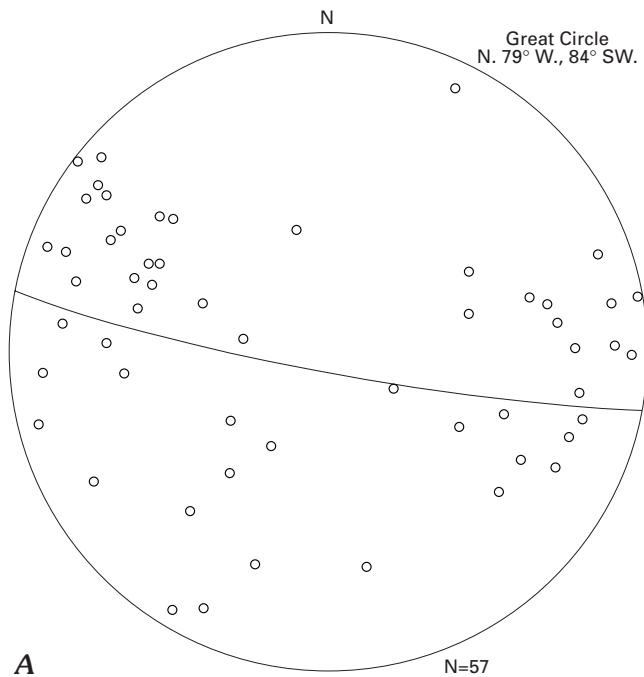
N

Great Circle
N. 79° W., 84° SW.

A   N=57

N

Mean=47° N. 67° E.

B   N=15

Figure 8. Equal-area projections (lower hemisphere) of
D_2 structures in Flattop Butte Granite. *A*, individual
plots of poles to S_2 schistosity. *B*, orientation of L_2
lineation, contoured; rare folds are oriented similarly to
lineations.

Rawhide Creek terrane is strongly deformed, locally to
mylonite. The S_2 foliation strikes northwest and dips steeply
except adjacent to the Little Wildcat Canyon fault, where it
strikes and dips subparallel to the fault. A rodding (stretch-
ing) lineation plunges moderately east to east-northeast, indi-
cating an anomalous west to southwest tectonic transport

direction at this locality during D_3 deformation. The folia-
tion adjacent to the fault is superposed on the regional north-
west-trending S_3 foliation only within a distance of 20–50 m
from the fault and is interpreted as a late S_3 surface. Dikes of
unit Xm in the foliated granite strike northwest and dip
steeply. They are deformed but less highly metamorphosed
than the mafic dikes in the Rawhide Buttes terrane.

MUSKRAT CANYON TERRANE

The Muskrat Canyon terrane consists largely of marble
and lesser amounts of quartzite, iron-formation, and con-
glomerate. The terrane is bounded on the west by the Little
Wildcat Canyon fault and on the east by the Muskrat Can-
yon fault. Asymmetric structures exposed in mylonite in the
Little Wildcat Canyon fault in the SW¼ sec. 33, T. 31 N., R.
64 W., indicate that rocks of the Muskrat Canyon terrane
have ridden upward and over the rocks in the Rawhide
Creek terrane. The dominant structures in the Muskrat Can-
yon terrane are northeast-trending folds (F_3) overturned to
the west and generally plunging northeast. The folds have
an axial planar foliation (S_3). The entire section is structur-
ally overturned. The folds in dolomite tend to be open
structures. A stretching lineation that plunges southeast
occurs locally in relatively high strain rocks. The rocks of
the terrane are interpreted as being allochthonous with
respect to the Rawhide Creek terrane.

WILDCAT HILLS TERRANE

The Wildcat Hills terrane is composed predominately
of mafic metavolcanic rocks, exposed at the mouth of Musk-
rat Canyon and on the eastern, lower slopes of the Wildcat
Hills. It composes the hanging wall of the Muskrat Canyon
fault, a northwest-verging ductile shear zone that was folded
(asymmetric S-folds) subsequent to its formation. The
metavolcanic rocks locally have a stretching (rodding) lin-
eation that plunges moderately southeast; accordingly, tec-
tonic transport during deformation D_3 was northwestward
relative to the metavolcanic rocks of the lower plate of the
Muskrat Canyon fault. Within Muskrat Canyon, local seg-
ments of the metavolcanic rocks are weakly deformed and
preserved pillow structures indicate that the volcanic suc-
cession is structurally inverted. Overturned pillow lavas are
best preserved in the north-central part of sec. 19, T. 30 N.,
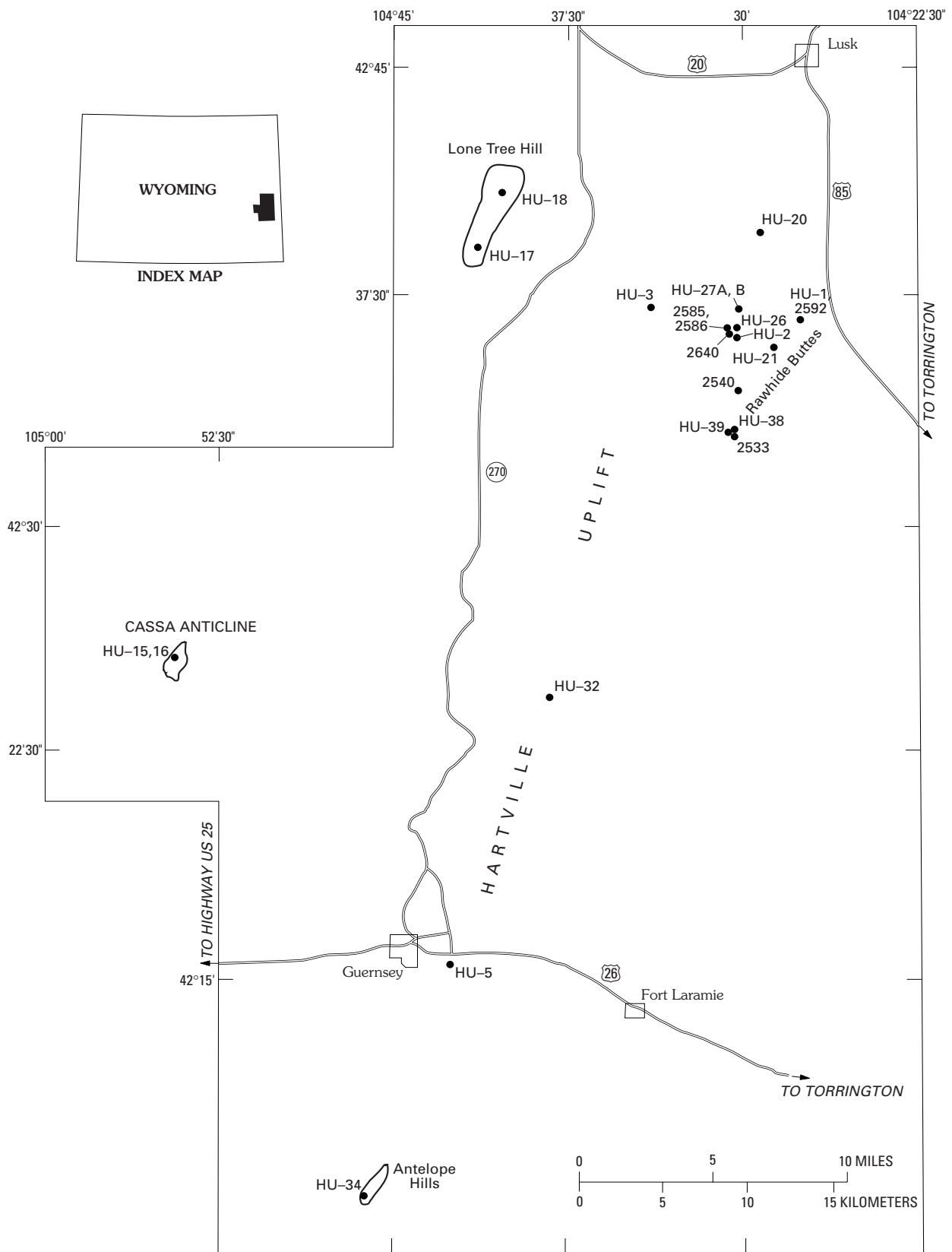R. 64 W., on the south side of Muskrat Creek.

8

Figure 9. Map showing localities of geochronology samples.

Table 4. *Rubidium and strontium data for whole-rock samples and minerals from the Flattop Butte Granite and the Rawhide Buttes Granite.*

[Suffix letters refer to type of sample: WR, whole rock; Mi, microcline; and Bi, biotite. Analytical uncertainties based on replicate analyses of Precambrian granitic rocks: ± 1.75 percent for $^{87}Rb/^{86}Sr$ and ± 0.025 percent for $^{87}Sr/^{86}Sr$ at the 95 confidence level. do, ditto]

Sample No.	Rock type	Concentration (parts per million)		$^{87}Rb/^{86}Sr$	$^{87}Sr/^{86}Sr$
		Rb	Sr		
Flattop Butte Granite					
HU–2 WR	Biotite-muscovite gneiss..............	227.9	54.53	12.59	1.1254
HU–26 WR	...do..............................	271.2	88.1	9.183	1.0217
HU–27A WR	...do..............................	243.6	98.01	7.383	0.9755
HU–27B WR	Aplite dike......................	177.8	25.67	21.35	1.3717
2586 WR	Biotite-muscovite gneiss..............	250.8	99.85	7.463	0.9804
2640 WR	...do..............................	261	70.54	11.11	1.0902
Rawhide Buttes Granite					
HU–1 WR	Biotite gneiss..............................	217.5	103.6	6.211	0.9361
HU–1 Mi	...do..............................	393.7	167	6.987	0.9539
HU–1 Bi	...do..............................	1087	11.97	516.4	10.566
HU–3 WR	...do..............................	219.2	86.95	7.497	0.9879
HU–3 WR	...do..............................	220	86.94	7.526	0.9878
HU–15 WR	...do..............................	154.3	149.3	3.023	0.8135
HU–20 WR	...do..............................	149.3	190.2	2.289	0.7833
HU–21 WR	...do..............................	128.5	216.6	1.728	0.7699
HU–38 WR	...do..............................	208.9	84.02	7.393	0.9845
HU–39 WR	...do..............................	291.6	122.1	7.071	0.9402
2533 WR	...do..............................	308.2	84.98	10.85	1.0505
2540 WR	...do..............................	227.1	192.3	3.458	0.8235
2562 WR	...do..............................	170.6	202.7	2.454	0.7862
2592 WR	...do..............................	228.3	97.76	6.923	0.9557
Miscellaneous samples					
HU–5 WR	Cataclastic gneiss........................	188.4	82.8	6.37	0.9304
HU–16 WR	Augen gneiss................................	99.12	178.2	1.62	0.7693
HU–17 WR	Biotite gneiss..............................	51.22	92.22	1.618	0.7718
HU–18 WR	...do..............................	164.6	76.33	6.365	0.7684
HU–32 WR	Garnet gneiss..............................	161.3	247.7	1.896	0.765
HU–34	Biotite gneiss..............................	62.96	112	1.637	0.7684

GEOCHRONOLOGY

By Z.E. Peterman, Kiyoto Futa, and R.E. Zartman

The two major granitic bodies in the map area, the Late Archean Flattop Butte Granite and the Late Archean Rawhide Buttes Granite, have been dated by the Rb-Sr whole-rock method. An outlying granite gneiss body, the gneiss at Cassa anticline (fig. 9), which possibly is grossly equivalent to the Rawhide Buttes Granite, has been dated by the U-Pb zircon method.

FLATTOP BUTTE GRANITE

The Flattop Butte Granite is a small body of deformed biotite-muscovite granite that intrudes garnet-biotite schist (unit Ws_1) and associated quartzite in the Flattop Butte terrane (fig. 4). It differs in composition from the nearby Rawhide Buttes Granite in that muscovite is a ubiquitous varietal mineral. Also, the Flattop Butte Granite is not cut by the amphibolite (unit Xm) dikes that are so abundant in the Rawhide Buttes Granite. Rb-Sr, U-Pb, and Sm-Nd ages for the Flattop Butte Granite are strongly disparate and reflect a complex history of the unit.
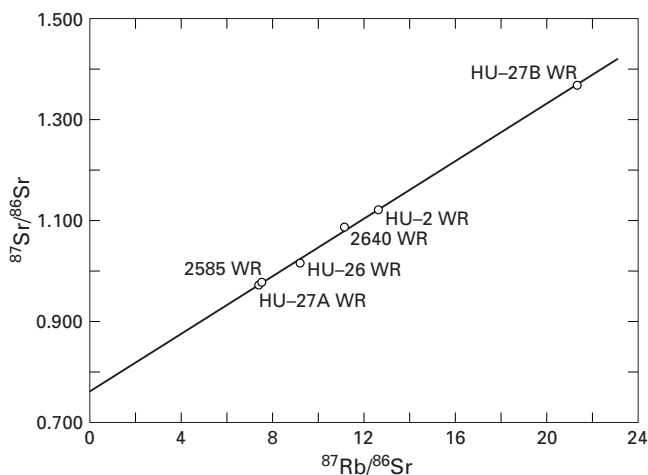
Figure 10. Rubidium-strontium isochron diagram for whole-rock samples of the Flattop Butte Granite. Isochron: 1.98±0.10 Ga and IR=0.767±0.016. Interpreted as age of metamorphism (D_2 deformation). Analytical data given in table 4.

Six samples of granite (table 4) define a Model III (MSWD = 3.87) Rb-Sr isochron (fig. 10; Ludwig, 1991) having an age of 1.98±0.10 Ga and an initial ratio (IR) of 0.767±0.009, which we interpret as the age of D_2 metamorphism. The uncommonly high IR indicates derivation of the granite from an older source, probably through anatexis.

Six samples analyzed by instrumental neutron activation show little variation in Sm/Nd ratios (table 5), and an isochron could not be generated. Four of these samples were analyzed by isotope dilution, and the data give model ages clustering around 3.0±0.1 Ga.

In an attempt to resolve the ambiguities in the Rb-Sr and Sm-Nd data, zircon from a 50-kg sample of HU–27A was analyzed (table 6). The zircons are strongly metamict.

They are greenish-gray, have a greasy luster, and are cloudy to nearly opaque in transmitted light. The crystal faces are pitted and etched, and some grains have been broken and recemented in misaligned orientations. All the zircons are to some degree magnetic. Small amounts of the least magnetic grains of the 100- to 200- and 325- to 400-mesh fractions were obtained at low amperage on the magnetic separator. Several milligrams were hand picked from these lesser magnetic fractions for analysis. These two fractions are extremely discordant in U-Pb ages and plot close together on a concordia diagram (fig. 11). The $^{207}Pb/^{206}Pb$ ages of 2.00 and 2.08 Ga are close to the Rb-Sr isochron age, but a chord passing through the two closely spaced data points has concordia intercepts of 0.37 and 2.80 Ga, the latter in approximate agreement with the Sm-Nd model ages.

We interpret these discordant ages as indicating that the Flattop Butte Granite was anatectically derived from a much older felsic source. The presence of both biotite and muscovite in the granite is consistent with its being an S-type (for example, Ferguson and others, 1980). In such crustally derived granites, Sm-Nd ages commonly reflect the age of the source material rather than the age of emplacement. For example, classical S-type granites of early Paleozoic age from southeast Australia have εNd values of –6.1 to –9.8 that reflect derivation of the magmas from a 1.4-Ga source (McCulloch and Chappell, 1982). If the Sm/Nd ratios of the Flattop Butte Granite were not fractionated during anatexis, the model ages of 3.0±0.1 Ga would be close to the age of the protolith (for example, DePaolo, 1981). The average Rb/Sr ratio of the source material would have to have been in the range of 0.4–0.7 in order to generate strontium having an $^{87}Sr/^{86}Sr$ of 0.767±0.009 at 1.98 Ga. Rb/Sr values in this range would indicate a protolith of granitic rock or one in which pelitic sedimentary rocks were abundant.

Table 5. *Samarium-neodymium data for whole-rock samples from the Hartville uplift.*

[Sm and Nd concentrations are precise to ± 1.5 percent (2 sigma). Uncertainties for $^{143}Nd/^{144}Nd$ are given as plus and minus values of the last one or two figures of the ratio. εo is [($^{143}Nd/^{144}Nd$–0.512636)/0.512636]×10^4. T_m (model age in 10^9 yrs) is (1/6.54×10^{-12})[1+$^{143}Nd/^{144}Nd$–0.512636)/($^{147}Sm/^{144}Nd$)], where 6.54×10^{-12} is the decay constant for ^{147}Sm in yr^{-1}. --, not determined]

Sample No.	Sm, ppm	Nd, ppm	$^{147}Sm/^{144}Nd$	$^{143}Nd/^{144}Nd$	εo	T_m (Ga)
			Rawhide Buttes Granite			
HU–20	7.16	36.6	0.119	0.511306	–25.9	2.6
			Flattop Butte Granite			
HU–2	5.59	30	0.1132	0.510981	–32.3	3
HU–26	9.49	51	0.1133	0.510892	–34	3.16
HU–27A	9.71	55.6	0.1063	0.510895	–34	2.92
HU–27B	2.52	14.9	0.103	0.510892	–34	2.82
[1]2585	9.1	52.5	0.106	--	--	--
[1]2640	9.2	49.7	0.113	--	--	--

[1]Instrumental neutron activation analyses for Sm and Nd. All others are by isotope dilution.

Table 6. *Uranium, thorium, and lead data for zircons from the Flattop Butte Granite and gneiss at Cassa anticline.*

[Numbers in parentheses below atom ratios, ages in millions of years. Numbers in parentheses after sample numbers are screen sizes of the zircons]

| Sample No.	Concentration (parts per million			Isotopic composition of lead (atom percent)				Atom ratios			
	U	Th	Pb	^{204}Pb	^{206}Pb	^{276}Pb	^{208}Pb	$\dfrac{^{206}\text{Pb}}{^{238}\text{U}}$	$\dfrac{^{207}\text{Pb}}{^{235}\text{U}}$	$\dfrac{^{207}\text{Pb}}{^{206}\text{Pb}}$	$\dfrac{^{208}\text{Pb}}{^{232}\text{Th}}$
Gneiss at Cassa anticline											
HU–16 (150–200)	3,015	1,552	620.9	0.718	45.19	15.99	38.10	0.0857 (530)	1.8738 (1,072)	0.1586 (2,440)	0.0656 (1,283)
HU–16 (325–400)	2,528	1,576	621.2	0.690	45.01	15.64	38.66	0.1028 (631)	2.2548 (1,198)	0.1591 (2,446)	0.0711 (1,388)
HU–16 (325–400) HF-leached	1,257	1,070	434.2	0.711	44.31	15.79	39.19	0.1405 (847	3.0889 (1,429)	0.1594 (2,450)	0.0724 (1,413)
HU–16 (325–400) HF-leachate	3,031	1,587	511.6	0.701	45.31	16.02	37.97	0.0708 (441)	1.6090 (974)	0.1646 (2,504)	0.0543 (1,069)
Flattop Butte Granite											
HU–27A (100–200) NM	1,165	1,001	198.3	0.359	60.80	12.55	26.29	0.1095 (670)	1.9378 (1,094)	0.1283 (2,075)	0.0309 (615)
HU–27A (325–400) NM	1,280	931	202.9	0.360	61.38	12.33	25.93	0.1030 (632)	1.7460 (1,026)	0.1229 (1,999)	0.0330 (656)
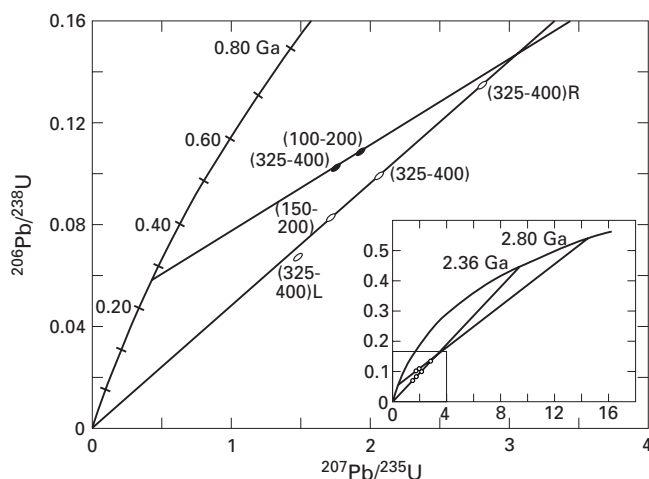
Figure 11. Uranium-lead concordia diagram for the zircons from the gneiss at Cassa anticline (HU–16, open symbols) and the Flattop Butte Granite (HU–27A, filled symbols). Numbers in parentheses are mesh size of zircon fractions. Suffix R identifies leached zircon; suffix L is leachate. The chord through the two points for HU–27A intersects concordia at 0.37±0.47 Ga and 2.80±0.17 Ga. The chord through the three points for HU–16 intersects concordia at 0.06±0.13 Ga and 2.36±0.17 Ga.

Figure 12. Rubidium-strontium isochron diagram for Rawhide Buttes Granite. Nine whole-rock sample data points were used in the regression: T=2.66±0.12 Ga and IR=0.696±0.009. Suffix letter abbreviations are the same as in table 4. The data point for HU–1 Bi is off scale, having coordinates at 516.4 and 10.566. The dot-dashed line is an isochron through HU–1 Bi, HU–1 Mi, HU-1 WR; T=1.32 Ga, IR=0.820. Analytical data given in table 4.

The U-Pb zircon data are consistent with the above interpretation. They could have been inherited from the source and then nearly completely reset at about 2.0 Ga, or they could have crystallized from the melt at this time and have incorporated some of the protolith zircons. The data show that the systems were strongly perturbed by the relatively recent loss of lead.
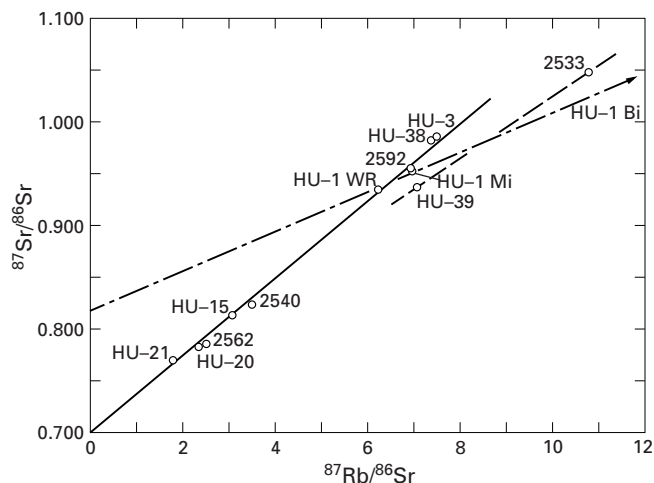
RAWHIDE BUTTES GRANITE

The Rawhide Buttes Granite crops out in Rawhide Buttes, the type area, and on the west side of the Hartville fault in the vicinity of Rawhide Creek. The granite is cut by abundant mafic dikes (unit Xm). Other bodies outside the map area, considered possible correlatives with the Rawhide Buttes Granite, crop out in outlying areas at Antelope Hills

(15 km south of Guernsey, figs. 1 and 9), Cassa anticline (23 km northwest of Guernsey), and Lone Tree Hill (18 km northwest of Rawhide Buttes). All of these bodies were sampled for rubidium and strontium analyses (table 4). Zircons were separated from samples of biotite gneiss at Cassa anticline (HU–16) and from a sample of the Rawhide Buttes Granite (HU–1). Those from sample HU–16 yielded only equivocal results (table 6). Zircons from HU–1 were considered to be too metamict to give meaningful results and were not analyzed.

Data for 9 of 12 samples of Rawhide Buttes Granite were used to construct a Rb-Sr whole-rock isochron having a Model III age (Ludwig, 1991) of 2.66±0.012 Ga and an IR of 0.696±0.009 (fig. 12). This array includes one sample from Cassa anticline (HU–15) that individually had a model age of 2.57 Ga. It is a fine- to medium-grained, foliated biotite granite that intrudes coarser grained, banded augen gneiss. Data for two samples from the southern end of Rawhide Buttes (HU–39 and 2533) plot considerably off the isochron (fig. 12) and were deleted from the regression. The scatter for the nine data points exceeds analytical error (MSWD = 27.3) and reflects open-system behavior of the whole-rock systems during younger metamorphism. The Model I (Ludwig, 1991) solution to the regression yields an age of 2.60±0.20 Ga and an IR of 0.700±0.009. The older age for the Model III regression results from the lower IR of 0.696±0.009. Although taken at face value, the IR of 0.696 alone is impossibly low for either a Late Archean crustal or mantle source, and the large uncertainty of 0.009 gives a range that is permissive with either source. For comparison, the model age of the centroid of the data array, the average of the nine points regressed, is 2.58 Ga at a model IR of 0.7012 using the calc-alkaline orogenic model of Peterman (1979).

Considering the strong penetrative deformation superimposed on the Rawhide Buttes Granite, the excessive scatter of the Rb-Sr whole-rock data is not surprising. Nonetheless, the isochron firmly establishes the age of the granite as Late Archean. A Sm-Nd model age of 2.60 Ga for sample HU–20 (table 5) lends additional confidence to the Rb-Sr isochron age.

Isotopic disturbance of the Rawhide Buttes Granite is also evident at the mineralogic scale. Biotite and microcline from HU–1 are on an isochron that includes the whole-rock point of 1.32 Ga (fig. 12). This age is the same as a K-Ar biotite age reported by Goldich and others (1966) for a sample of the Haystack Range Granite at the south end of the uplift (Casebier Hills quadrangle). These biotite ages reflect a regional but geologically cryptic event that is recognized throughout the Archean terrane of southern Wyoming (Peterman and Hildreth, 1978).

Three samples of medium- to coarse-grained biotite gneiss from outlying areas (HU–16, HU–17, and HU–34; table 4) have greatly different Rb and Sr contents but nearly identical Rb/Sr ratios. At Cassa anticline (fig. 9), the gneiss

(HU–16) is intruded by foliated granite (HU–15) that probably correlates with the Rawhide Buttes Granite. Thus, the gneiss is older than about 2.66 Ga, and model ages for the three biotite gneiss samples range from 2.85 to 3.03 Ga. A fourth sample of gneiss from Lone Tree Hill (HU–18, table 4; fig. 9) contains more rubidium and less strontium and gives a much younger model age of 2.26 Ga. The sample appears to have been sheared and recrystallized, and the age has been partially reset.

Zircons from HU–16 were analyzed (table 6) in an attempt to verify the 2.9 Ga Rb-Sr model age for the gneiss at Cassa anticline. The zircons are strongly metamict but appear to consist of a single population of types varying mainly in color and clarity. They range from light-colored translucent to dark-brown, nearly opaque variants. Faces are badly pitted, and face edges have been rounded. In transmitted light, the grains are cloudy, locally contain opaque inclusions, and are extensively fractured. Iron staining along fractures is common. Extinction is uneven and spotty as though individual grains comprise many small domains of differing optical character. The uranium-lead ages are extremely discordant (table 6, fig. 11), and common-lead contents are quite high. Hand-picked separates of 150–200 and 325–400 mesh were initially analyzed. The finer fraction was leached with cold 10 percent HF to determine if soluble, high-lead phases or domains may have been present. The leaching did not appreciably change the lead isotopic composition in the zircon, but uranium was reduced by 50 percent and thorium by 30 percent. Thus, the zircons contain very high uranium and thorium domains that are extremely discordant. Because of the high common-lead content, the isotopic composition used for the common-lead correction is critical. The data plotted on the concordia diagram (fig. 11) are based on a modern common-lead correction using values of Stacey and Kramers (1975). Intercepts are at 2.36±0.17 Ga and nearly 0. A 3.0-Ga common lead would produce a chord having an upper intercept of 2.46 Ga. In both cases, the upper intercept age is anomalously young because other data show that the gneiss is at least Late Archean, possibly 2.9 Ga or older.

The anomalously high common-lead content and the discordance pattern are problematical. We cannot determine from the isotopic data when the zircon incorporated the large amounts of common lead, but it is unlikely that this occurred during magmatic crystallization. Further complications are indicated by Th-Pb ages (table 6) that cannot be explained by non-fractionating lead loss or by the leaching experiment that resulted in preferential dissolution of uranium- and thorium-enriched phases. We conclude that this complex post-crystallization history precludes derivation of meaningful age information from these highly metamict zircons.

13

REFERENCES CITED

Chappell, B.W., and White, J.R., 1974, Two contrasting granite types: Pacific Geology, v. 8, p. 173–174.

———1992, I- and S-type granites in the Lachlan Fold Belt, *in* Brown, P.E., and Chappell, B.W., eds. Second Hutton Symposium on the Origin of Granites and Related Rocks: Transactions of the Royal Society of Edinburgh, v. 83, part 1, p. 1–26.

Dahl, P.S., and Frei, Robert, 1998, Step-leach Pb-Pb dating of inclusion-bearing garnet and staurolite, with implications for Early Proterozoic tectonism in the Black Hills collisional orogen, South Dakota, United States: Geology, v. 26, no. 2, p. 111–114.

Day, W.C., Sims, P.K., Snyder, G.L., and Wilson, A.B., 1994, Hartville Uplift, southeastern Wyoming—Revisited: Geological Society of America Abstracts with Programs, v. 26, no. 6, p. 10.

DePaolo, D.J., 1981, Neodymium isotopes in the Colorado Front Range and crust-mantle evolution in the Proterozoic: Nature, v. 21, p. 193–196.

Ferguson, John, Chappell, B.W., and Goleby, A.B., 1980, Granitoids in the Pine Creek geosyncline, *in* Proceedings of International Symposium on the Pine Creek geosyncline: International Atomic Energy Agency, p. 73–90.

Goldich, S.S., Lidiak, E.G., Hedge, C.E., and Walthall, F.G., 1966, Geochronology of the mid-continent region, United States—2, Northern area: Journal of Geophysical Research, v. 71, p. 5389–5408.

Jones, D.L., Silberling, N.J., and Hillhouse, J.W., 1977, Wrangellia—A displaced terrane in northwestern North America: Canadian Journal of Earth Sciences, v. 14, p. 2565–2577.

Krugh, K.A., Chamberlain, K.R., and Frost, C.D., 1996, Post-Cheyenne belt thermotectonism on the eastern margin of the Wyoming Province—Hartville Uplift, SE Wyoming: Geological Society of America Abstracts with Programs, p. A–315.

Lewry, J.F., Lucus, S., Stern, R., Ansdell, K., and Ashton, K., 1996, Tectonic assembly and orogenic closure in the Trans-Hudson orogen: Geological Association of Canada Programs with Abstracts, v. 21, p. A56.

Ludwig, K.R., 1991, Isoplot, a plotting and regression program for radiogenic isotope data: U.S. Geological Survey Open-File Report 91–445, 45 p.

McCulloch, M.T., and Chappell, B.W., 1982, Nd isotopic characteristics of S- and I-type granites: Earth and Planetary Science Letters, v. 58, p. 51–64.

Peterman, Z.E., 1979, Strontium isotope geochemistry of Late Archean to Late Cretaceous tonalites and trondhjemites, *in* Barker, Fred, ed., Trondhjemites, dacites, and related rocks: New York, Elsevier Scientific Publishing Company, p. 133–147.

Peterman, Z.E., and Hildreth, R.A., 1978, Reconnaissance geology and geochronology of the Precambrian of the Granite Mountains, Wyoming: U.S. Geological Survey Professional Paper 1055, 22 p.

Redden, J.A., and Dewitt, Ed, 1996, Early Proterozoic tectonic history of the Black Hills—An atypical Trans-Hudson orogen: Geological Society of America Abstracts with Programs, p. A–315.

Redden, J.A., Peterman, Z.E., Zartman, R.E., and DeWitt, Ed, 1990, U-Th-Pb geochronology and preliminary interpretation of Precambrian tectonic events in the Black Hills, South Dakota, *in* Lewry, J.F., and Stauffer, M.R., eds., The Early Proterozoic Trans-Hudson Orogen of North America: Geological Association of Canada Special Paper 37, p. 229–251.

Resor, P.G., Chamberlain, K.R., Frost, C.D., Snoke, A.W., and Frost, B.R., 1996, Direct dating of deformation—U-Pb age of syndeformational sphene growth in the Proterozoic Laramie Peak shear zone: Geology, v. 24, p. 623–626.

Sims, P.K., Day, W.C., Snyder, G.L., and Wilson, A.B., 1997, Geologic map of Precambrian rocks along part of the Hartville Uplift, Guernsey and Casebier Hill quadrangles, Platte and Goshen Counties, Wyoming, *with a section on* Geochronology of post-tectonic intrusive rocks by Z.E. Peterman: U.S. Geological Survey Miscellaneous Investigations Series Map I–2567, scale 1:24,000.

Sims, P.K., and Peterman, Z.E., 1986, Early Proterozoic Central Plains orogen—A major buried structure in the north-central United States: Geology, v. 14, p. 488–491.

Sims, P.K., Peterman, Z.E., Hildenbrand, T.G., and Mahan, Shannon, 1991, Precambrian basement map of the Trans-Hudson orogen and adjacent terranes, northern Great Plains, U.S.A.: U.S. Geological Survey Miscellaneous Investigations Series Map I–2214, scale 1:1,000,000; includes pamphlet, 53 p.

Smith, W.S.T., 1903, Hartville Folio: U.S. Geological Survey Folio No. 91.

Snyder, G.L., 1980, Map of Precambrian and adjacent Phanerozoic rocks of the Hartville Uplift, Goshen, Niobrara, and Platte Counties, Wyoming: U.S. Geological Survey Open-File Report 80–779, scale 1:48,000.

Stacey, J.S., and Kramers, J.S., 1975, Approximation of terrestrial lead isotope evolution by a two stage model: Earth and Planetary Science Letters, v. 26, p. 207–221.